JOURNAL OF CATALYSIS 31, 325–334 (1973)

Hydrogen Adsorption on High Surface Area Platinum Crystallites

K. KINOSHITA, J. LUNDQUIST, AND P. STONEHART

Materials Engineering and Research Laboratory, Pratt & Whitney Aircraft, Middletown, Connecticut 06457

Received February 14, 1972

Quasi-equilibrium hydrogen adsorption isotherms are obtained on a series of high surface area platinum catalysts supported on graphitized carbon using a linear perturbation electrochemical technique. This technique gives a rapid determination of the platinum catalyst surface area (and hence crystallite size) and gives fine resolution of the isotherms due to the individual surface hydrogen species. The two major adsorbed hydrogen species, "weakly" and "strongly" bonded, are observed on both deposition and oxidation of the adsorbed hydrogen. In addition, a "third" minor species is observed during oxidation when both major species are present. It is shown that this "third" species is a surface entity rather than an artifice due to hydrogen atoms dissolved in the platinum metal or hydrogen molecules dissolved in the catalyst pore structure, probably arising from an interaction between the two major adsorbed species. Surface coverages by this "third" species are dependent upon the platinum crystallite size, being negligible on low surface area crystallites. It has not been determined whether the platinum crystallite size effect on the hydrogen adsorption isotherms is due to a changing surface morphology or material state as the crystallite size decreases.

INTRODUCTION

An examination of adsorption isotherms and the related kinetics of adsorption/desorption for reacting molecules on catalyst surfaces has been one of the focal points for interpreting catalytic mechanisms and the relative importance of reaction intermediates. Recently (*1–7*), linear perturbation techniques have been developed whereby a dynamic adsorption/desorption parameter is examined. This measurement is, of course, the first differential of the static adsorption isotherm, assuming quasi-equilibrium conditions. In gas phase catalysis the catalyst temperature is varied as a linear function with time and analyses of the rate of desorption for the adsorbed species are carried out by analyzing with a mass-spectrometer or microbalance. Owing to difficulties in control and detection, the fine resolution needed to resolve the effects of surface interactions on the isotherms has not been obtained. In a related manner, changing the surface free energy of the catalyst by varying the electrochemical potential as a linear function with time gives (*5–7*) kinetics of reactive adsorption/desorption with fine resolution; as the net electron change is easily monitored as a reaction parameter.

Adsorption of hydrogen on platinum catalysts has been studied by several groups (*3*, *7–9*) using related linear perturbation techniques, latterly (*8*) deriving the specific oxidation and deposition rate parameters. At room temperature in the gas phase, hydrogen is chemisorbed on platinum as atoms, with one hydrogen atom associated with each surface platinum atom. The surface equilibrium constant between hydrogen molecules and atoms is very small ($K = \mathrm{Pt{\cdot}H_2/Pt{\cdot}H{\cdot}}$) and the kinetics of hydrogen molecule dissociation are very fast. Any discussion of adsorption isotherms, therefore, refers to equilibrium concentrations of hydrogen atoms on the

platinum catalyst surfaces. In the electrochemical case, chemisorbed hydrogen atom coverages are observed at negligible partial pressures of hydrogen and it is the potential dependent surface equilibrium coverages of chemisorbed hydrogen atoms that are discussed here. Two distinct forms of adsorbed hydrogen atoms on platinum have been observed (*3, 7, 9–14*). These are designated as "weakly" and "strongly" bonded hydrogen. In addition, a third minor intermediate species has been observed during potentiodynamic anodic oxidation of the adsorbed hydrogen, which is not observed on cathodic hydrogen deposition under quasi-equilibrium conditions. Will (*11*) suggested that the third species arises from hydrogen adsorption on the Pt(111) face, whereas Stonehart (*7*) suggested that this species results from a surface interaction between the "strongly" and "weakly" bonded hydrogen forms. Breiter (*15*), on the other hand, interpreted this apparent third species as arising from the oxidation of hydrogen atoms and molecules diffusing to the platinum surface from the interior of the metal and the solution during the linear perturbation.

Hydrogen adsorption on platinum single crystals (*11*) and on platinum with different (*16*) degrees of dispersion has been investigated previously. The concentration ratios of "strongly" to "weakly" bonded hydrogen vary with the platinum crystal face and this was applied by Stonehart and Zucks (*17*) to interpret changes in the surface morphology of unsupported platinum black crystallites (40–10 m^2/g Pt) during sintering in concentrated phosphoric acid at 135°C. Distinct changes in the character of the hydrogen adsorption isotherm were noted as the platinum crystallites grew, so a detailed examination of the quasi-equilibrium behavior and *inter alia* the interaction changes for adsorbed hydrogen on high surface area platinum crystallites is presented here. Using a variety of small platinum crystallite sizes, the surface to volume ratios may be changed to examine the contributions of internally dissolved hydrogen in the platinum crystallites to the experimental potentiodynamic adsorption/desorption isotherms.

Deconvolution Analysis

The fundamental equations and numerical solutions for the reaction rate/time characteristics of adsorbed species with linear perturbations of temperature or surface free energy have been described previously (*2, 5–7, 18*). When the rate of attainment of surface equilibrium is greater than the perturbation rate, quasi-equilibrium conditions are obtained and in the electrochemical case, the surface ratio of covered to uncovered sites is given by

$$\frac{1-\theta}{\theta} = K \exp \frac{VFn}{RT} \cdot \exp 2g\theta. \qquad (1)$$

In cases where both the reactant and product are specifically adsorbed, θ is the surface coverage by the reactant but in the case of adsorbed hydrogen atoms on platinum, θ is the surface coverage of hydrogen atoms and $(1 - \theta)$ represents the nonadsorbed hydrogen atom sites. The sites are not bare, as solvent molecules are present (water) but they may be treated as bare for the purposes of isotherm and kinetic evaluations. V is the electrode potential; n the number of equivalents per mole of reactant; K the ratio of the forward rate constant, k_a, to the reverse rate constant k_c, ($K = k_a/k_c$) and g is the heterogeneity parameter denoting the degree of departure from the Langmuir adsorption isotherm due to surface heterogeneity or interaction (*7*). F, R and T are the usual electrochemical constants. With a linear potential perturbation ($dV/dt = v, V/s$) the reaction rate to maintain equilibrium is recorded as a current density.

$$\frac{i}{A} = f(d\theta/dV) \cdot v. \qquad (2)$$

The action of the heterogeneity parameter on the normalized reaction rate/electrode potential (or time) parameter is shown in Fig. 1. As quasi-equilibrium is maintained, the peaks are symmetrical and become progressively broader with increase

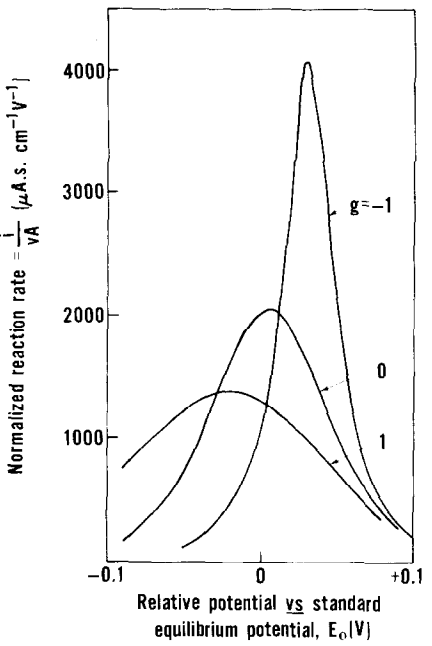

FIG. 1. Quasi-equilibrium current/potential profiles for different heterogeneity parameter values. $K = 1.0$, $\theta_{initial} = 1.0$.

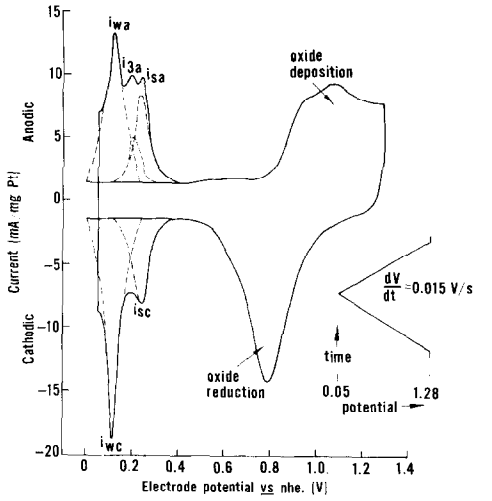

FIG. 2. Potentiodynamic current/potential profile for 67 m^2/g Pt on graphitized carbon. Construction of deconvolution profiles for the adsorbed hydrogen species. 1 M H_2SO_4 v = 0.015 V/s.

in g. The peak width at half-height is diagnostic of the magnitude of the heterogeneity parameter, giving 0.148, 0.090 and 0.038 V for $g = 1.0$, 0.0 and -1.0, respectively. Reaction orders different from unity are not considered as they may not be separated numerically from the heterogeneity parameter.

Since adsorbed hydrogen on platinum shows two major coexisting species, the composite reaction rate/electrode potential appears as two overlapping peaks on hydrogen deposition and three overlapping peaks on oxidation (Fig. 2). Approximate solutions of isotherm parameters for the two major adsorbed hydrogen species were described by Breiter (*13*, *14*), using both Langmuir and Frumkin isotherms. Exact solutions were obtained by Stonehart (*7*) using convergence routines on a computer, varying the heterogeneity parameter g in Eq. (1). Franklin *et al.* (*19*) examined the adsorbed hydrogen coverage on platinum as a function of potential and approximated the reaction rate peaks as simple triangles, calculating the overlap for only the two major adsorbed hydrogen forms. Deconvolution of the reaction peak profiles did not require the detailed computer processing demonstrated previously (*7*) but did require more exact separations than may be obtained by simple triangular approximations. For a graphical analysis of the parameters in the adsorbed hydrogen isotherms, it is assumed that the "strongly" bonded (peak maximum at +0.24 V vs nhe) cathodic hydrogen is formed reversibly with a symmetrical current/potential profile about the current maximum. This is subtracted from the overall cathodic deposition current to yield the current/potential profile for the "weakly" bonded hydrogen; also symmetrical about the current maximum (+0.12 V vs nhe). Drawing a symmetrical peak, it is apparent that saturation of the platinum surface with adsorbed hydrogen occurs at 0.0 V vs nhe ($\theta = 1.0$). The anodic peaks are constructed by assuming the "strongly" bonded species to have a mirror image current/potential profile to the cathodic deposition. The "weakly" bonded species is constructed by drawing a symmetrical peak about the current maximum with the base line extending

to 0.0 V vs nhe. Subtraction of the coverages due to the two constructed peaks from the measured convoluted profile gives rise to a residual "third" peak, shown in Fig. 2.

In this analysis, the formation of molecular hydrogen was considered negligible at potentials greater than 0.05 V, so this contribution to the total current was not included. It is now possible to identify the contributions of hydrogen surface species to the total coverage and determine the factors giving rise to this "third" species as a function of the crystallite size. This analysis also supports the view that the "weakly" adsorbed hydrogen on deposition gives rise to the charge associated with the third anodic peak as this species cannot be observed until both the strongly and weakly bonded hydrogen forms are present (*7*).

Experimental Details

High surface area platinum crystallites were supported on graphitized carbon black to maintain electrical integrity and separate the individual crystallites. The catalysts were prepared by impregnating the graphitized carbon blacks with solutions of platinum diammino dinitrite in nitric acid, in sufficient proportions to give the desired platinum loadings. The slurries were slowly reduced to dryness and the platinum salt decomposed to the metal and metal oxide by heating in air at 500°C for 2 hr. These catalysts were fabricated into PtFe-bonded electrodes (*20*) with a minimum of PtFe (<7 wt %) to maintain structural integrity. The platinum catalyst electrodes were placed in a conventional three compartment cell and a periodic triangular potential sweep was applied to a Wenking potentiostat from a Hewlett-Packard 202A function generator. The electrolyte was 1 *M* H_2SO_4 saturated with nitrogen.

Platinum catalyst surface areas (and hence crystallite sizes) were determined from the total coulombic charge required for hydrogen deposition, after correcting for double layer charging, using 210 μC/real cm^2 Pt (*21*). This corresponds to 1.305×10^{15} atoms/cm^2 and assumes each surface platinum atom accommodates one hydrogen atom.

The platinum crystallite size was varied by inserting electrodes containing the smallest crystallites into hot concentrated phosphoric acid for short time periods and allowing sintering to take place, producing a wide range of platinum crystallite sizes in a controlled manner.

In order to insure that the supported catalysts were totally wetted by the electrolyte, the electrodes were immersed in concentrated nitric acid for 1 min, washed thoroughly with distilled water and inserted into the measuring cell. Hydrogen was evolved at -0.05 V vs nhe for 1 min and then the electrode potential was set to 1.3 V to oxidize the hydrogen in the porous electrode structure. This was repeated 2–3 times and gave reproducible current/potential curves on scanning between 1.28 and 0.05 V vs nhe at 0.015 V/s.

Results and Discussion

The characteristic potentiodynamic current/potential profile for high surface area platinum supported on graphitized carbon is shown in Fig. 2. The main criterion of quasi-equilibrium is maintained for the adsorbed hydrogen species in that the peak potentials for both oxidation and deposition are coincident. Therefore, kinetic or mass transport effects are absent. The same cannot be said for the oxygen deposition and reduction profiles where considerable asymmetry is seen, indicative of kinetic and surface rearrangement limitations (*6*). Figure 3 compares the potentiodynamic profiles for hydrogen deposition and oxidation on a series of platinum catalysts with varying areas but with the same metal content. It can be seen that the character of the composite oxidation peaks changes with the crystallite size and that the *total* oxidation/deposition charge decreases as the crystallite size increases (surface area decreases), as expected. It is clearly evident that three anodic hydrogen peaks are present. These anodic current peaks will be designated as the strongly bonded i_{sa}, weakly bonded i_{wa} and the intermediate third maximum i_{3a}. The strongly and weakly bonded cathodic current peaks will be designated as i_{sc} and i_{wc}, respectively. The

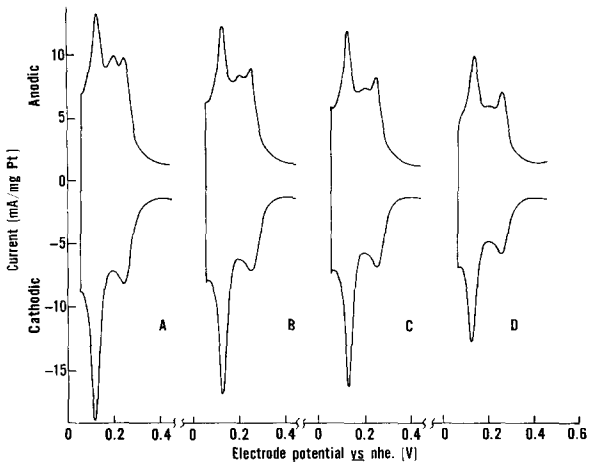

FIG. 3. Potentiodynamic current/potential profiles for hydrogen deposition and oxidation on 1.37 mg Pt catalysts supported on graphitized carbon. (A) 67; (B) 57; (C) 52, and (D) 42 m^2/g Pt. 1 M H_2SO_4 23°C; v = 0.015 V/s.

third anodic maximum i_{3a} appears to be disappearing as the surface area decreases, and correspondingly the strongly bonded anodic hydrogen peak becomes more pronounced. The rates at which the hydrogen adsorption/desorption current maxima change with Pt surface area is shown in Fig. 4a. In all instances, the current peak heights change linearly with the platinum catalyst surface areas. The results are normalized to the 67 m^2/g Pt catalyst in Fig. 4b for the fractional change in peak height as a function of the platinum catalyst surface area. The fractional changes of the i_{sc}, i_{wc} and i_{wa} all appear to lie within a band, changing by the same magnitude as the surface areas change. It can be seen from Fig. 4 that the third anodic

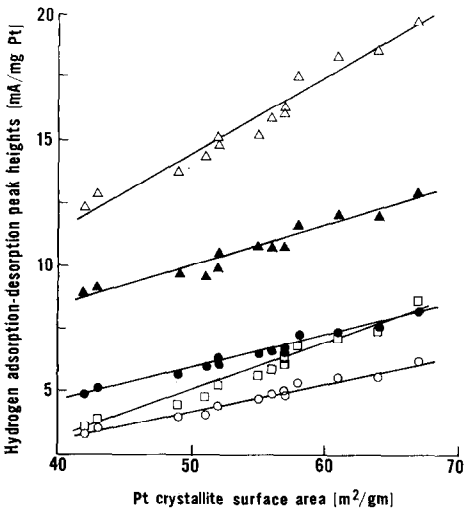

FIG. 4a. Potentiodynamic current peak heights for hydrogen oxidation and deposition on platinum crystallites supported on graphitized carbon. (○)i_{sc}; (△)i_{wc}; (□)i_{3a}; (●)i_{sa} and (▲)i_{wa}. 1 M H_2SO_4 23°C; 1.37 mg Pt/electrode; v = 0.015 V/s.

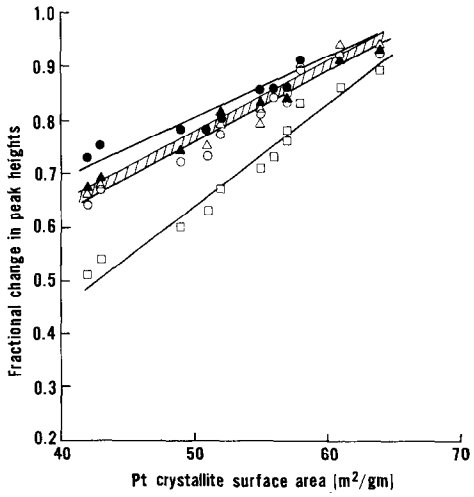

FIG. 4b. Current peak heights from Fig. 4a normalized to the 67 m^2/g Pt catalyst datum to compare relative changes with platinum crystallite sizes.

peak (i_{3a}) undergoes the greatest decrease in magnitude with decrease in the platinum surface area.

The coulombic charges associated with the different forms of adsorbed hydrogen were obtained by integrating the current/potential curves shown in Fig. 3. The quantities of adsorbed hydrogen in the different forms are plotted as a function of surface area in Fig. 5a. When the decrease in the amount of adsorbed hydrogen present in the different forms is plotted as a fractional change, normalized to the 67 m^2/g Pt catalyst, the curves in Fig. 5b are obtained. A comparison of Figs. 4 and 5 indicates that when either the current peak height or the charge is measured, a linear dependence with surface area is obtained. Since the current peak height is not necessarily indicative of the *amount* of adsorbed hydrogen the charge is the reliable measurement of the coverage by a given species.

As the platinum catalyst surface area is calculated from the total coulombic charge required for hydrogen deposition or oxidation, then a comparison of the influence of the crystallite size on the relative populations of the two major species is possible. It was found that the crystallite size

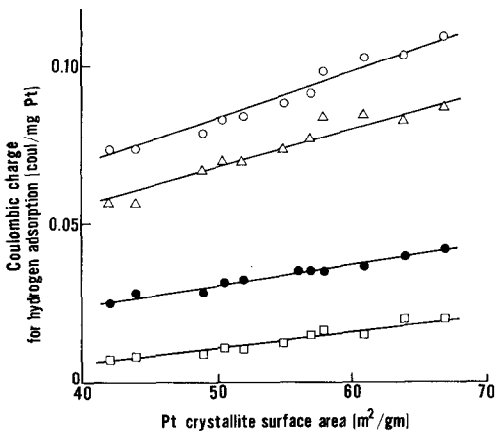

FIG. 5a. Potentiodynamic charges for surface species observed during hydrogen oxidation and deposition on platinum crystallites supported on graphitized carbon. (○)Q_{wc}; (●)$Q_{sc} = Q_{sa}$; (△)Q_{wa}; (□)Q_{3a}. 1 M H_2SO_4 23°C; 1.37 mg Pt/electrode; v = 0.015 V/s.

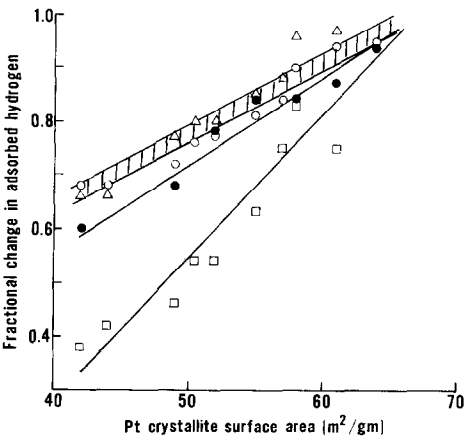

FIG. 5b. Charges for the surface hydrogen species on platinum from Fig. 5a normalized to the 67 m^2/g Pt catalyst datum to compare relative changes with platinum crystallite sizes.

did not affect the charge ratios (Q_{sc}/Q_{wc}) which were constant at 0.33 for the surface area range between 67 and 6 m^2/g Pt.

An examination of the peak widths at half-height did not show large differences in the heterogeneity parameter values for different crystallite sizes but did show differences between the species as shown in Table 1. The limits of error are inevitably quite large (± 0.2) but the values for the weak anodic species are uniformly greater than the heterogeneity parameters for the other species. In addition, all of the values indicate anti-Temkin adsorption (7). Although the heterogeneity parameter is generally considered to be a contribution from the catalyst morphology or "active sites," it can be seen from the values above, that for each individual surface species the heterogeneity parameters are insensitive to the crystallite sizes. These values can be

TABLE 1

Pt Crystallite surface area (m^2/g)	Heterogeneity parameter, g. sc	wc	wa	3a
67	−0.6	−0.6	0.0	−0.5
57	−0.6	−0.6	−0.2	−0.6
52	−0.4	−0.7	−0.2	−0.5
42	−0.4	−0.5	−0.2	−0.7

compared to previously reported heterogeneity parameter values (7) on smooth platinum but in a different ionic environment. It is concluded, therefore, that the heterogeneity parameter, g, is an extrinsic factor associated with the specific adsorbed species and is sensitive to any coadsorbed species, rather than an intrinsic function of the platinum crystallite surfaces. As such, the departure from ideal Langmuirian behavior is induced by interactions between the adsorbed species.

The magnitude of the third anodic current maximum is strongly dependent on the amount of adsorbed hydrogen present on the platinum surface. Figure 6 shows that as the hydrogen coverage increases to those values where weakly bonded hydrogen is present, the third anodic current maximum progressively appears. Because the third anodic peak does not have a corresponding "mirror image," a mechanism must be proposed to account for it and to give a physical interpretation. Figure 7 shows two restricted potentiodynamic scans on a platinum catalyst. In one instance the total hydrogen oxidation/deposition profile is recorded and in the other instance, only the profile due to the weakly bonded species recorded. In the latter case, the anodic and cathodic coulombic charges for the weakly bonded species are comparable; whereas, the corresponding charges for this species in the former case, obtained in the same potential region, are not. The hatched out area shows the difference between the two scans and corresponds to the charge

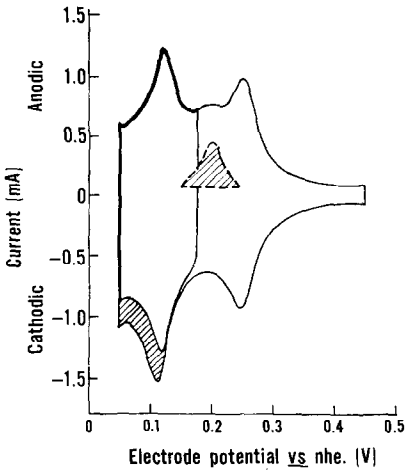

FIG. 7. Potentiodynamic scans for hydrogen oxidation and deposition on 30 m^2/g Pt crystallites. Comparison of the profile obtained for complete deposition and removal of all hydrogen species to the corresponding profile obtained for the weakly bonded species alone. Hatched areas indicate the contribution of the "third" interaction species. 1 M H_2SO_4 23°C; v = 0.027 V/s 0.11 mg Pt/electrode.

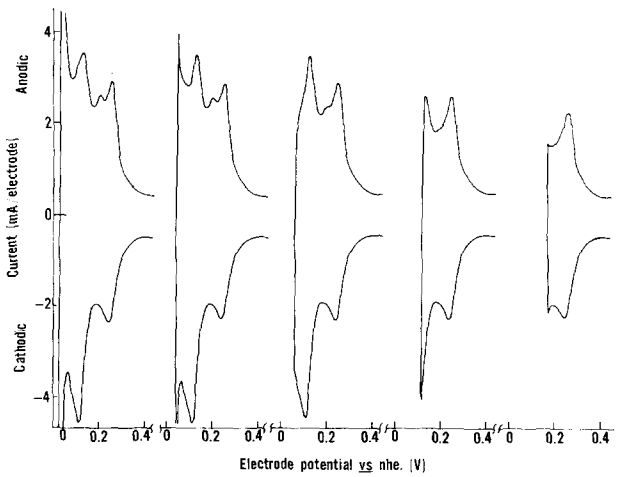

FIG. 6. Potentiodynamic current/potential profiles for hydrogen oxidation and deposition on 42 m^2/g Pt crystallites supported on graphitized carbon. Variation of the lowest hydrogen deposition potential changing the production of the "third" peak which influences the observed current peak height for oxidation of the strongly bonded species. 1 M H_2SO_4 23°C; 0.25 mg Pt/electrode; v = 0.025 V/s.

associated with the third anodic maximum. This shows that the coulombic contributions to the third anodic peak arise from part of the cathodic deposition charge associated with the weakly bonded hydrogen species. Due to the overlap between the anodic peak associated with the strongly bonded species and the third anodic peak, progressive formation of the latter phenomenologically increases the observed anodic peak height of the strongly bonded species. The relative influence and production of the third peak can be monitored from the changes in the strongly bonded cathodic/anodic peak height ratios. This is shown in Fig. 8 as a function of the lowest potential for hydrogen deposition during the potential scan (cf. Fig. 5). It is clear that a crystallite size effect is observed, with the highest surface area catalysts showing the greatest influence from the "third" peak.

Breiter (*15*) suggested the third anodic maximum arises from oxidation of dissolved atomic hydrogen in the platinum crystallite and molecular hydrogen dissolved in the electrolyte, both species being formed during the cathodic sweep. The magnitudes of the oxidation currents anticipated from these dissolved species can be determined for the catalysts used in this investigation. Assuming that the platinum particles are

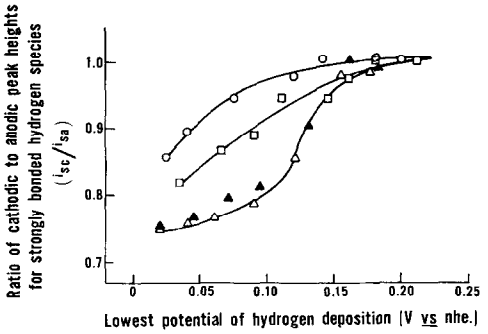

FIG. 8. Changes in the potentiodynamic current peak height ratios for the strongly bonded hydrogen species (i_{sc}/i_{sa}) on different platinum crystallite sizes; experimentally changing the lowest hydrogen deposition potential. (cf. Fig. 6). 1 *M* H_2SO_4 23°C; v = 0.023 V/s. (▲) 70; (△) 41; (□) 25 m^2/g Pt crystallites. (○) Pt flat sheet.

interstitially saturated with atomic hydrogen, then from the mass of platinum and the solid solubility of hydrogen in platinum the coulombic charge for oxidation of the dissolved hydrogen can be calculated. The data in Fig. 3 are obtained on 1.37 mg Pt and with a maximum hydrogen solubility (*21*) in the metal of $C_{H.(25)} = 2.2 \times 10^{-5}$ moles H·/cm^3, this accounts for 1.4×10^{-4} C for each electrode. This is less than 1% of the charge measured for the third anodic hydrogen peak on the 67 m^2/g Pt catalysts. The third anodic hydrogen peak accounts for 2.8×10^{-2} C/electrode.

Similarly, the total amount of dissolved hydrogen in the 1 *M* H_2SO_4 contained within the electrode structure can be calculated. For these electrodes, the electrolyte-take-up volume (ETU) is a measure of the pore volume, typically 1.5×10^{-2} cm^3/electrode. At 0.05 V the partial pressure of hydrogen is 0.02 atm giving a solubility of 1.3×10^{-8} moles H_2/cm^3. The coulombic charge to oxidize this hydrogen corresponds to 3.9×10^{-5} C/electrode. This is less than 0.1% of the charge measured for the third anodic hydrogen peak on the 67 m^2/g Pt catalyst.

The existence of the third anodic maximum cannot be attributed to a bulk concentration effect and must, therefore, be a surface phenomenon. Whether it is an intrinsic artifact of the surface morphology as the crystallite size changes or a surface interaction between the two major adsorbed species cannot be determined at this time but the latter is most likely.

A comparison of the charges associated with the cathodic deposition of the weakly bonded species and the sum of the charges associated with the anodic oxidation of the weakly bonded species and the "third" species gave an equivalence (±5%) for all catalysts. The ratio of the amount of hydrogen associated with the third anodic maximum (Q_{3a}) to the total hydrogen oxidation $(Q_a)_T$ decreases as a function of platinum surface area (Fig. 9). The results shown in Fig. 9 for the Pt surface areas of 25 and 6 m^2/g were obtained on Pt black, where the charge associated with the third anodic maximum becomes a smaller frac-

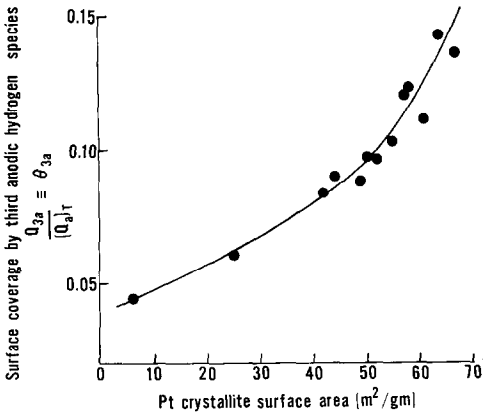

FIG. 9. Change in the fractional coverage due to the "third" hydrogen species as a function of the platinum crystallite size. 1 M H_2SO_4 23°C; v = 0.015 V/s.

tion of the total oxidized hydrogen on decreasing the platinum surface area. This suggests perhaps that the crystal structures of small platinum particles may play an important rôle in the surface interactions of adsorbed hydrogen.

There is a problem associated with the recording of hydrogen adsorption isotherms by potentiodynamic scanning which is not amenable to instrumental analysis. That is, during the cathodic sweep the strongly bonded hydrogen is first adsorbed, then as the potential further decreases the weakly bonded hydrogen is adsorbed. In the meantime the strongly bonded hydrogen may be undergoing surface diffusion and reorientation which cannot be easily measured. The diffusion and reorientation of adsorbed hydrogen may be a function of crystallite geometry and orientation but this dependence has not been examined.

It is recognized that the electrochemical perturbation techniques used here to examine the hydrogen atom oxidation/deposition parameters on platinum utilize a reactive electron transfer mode:

$$H\cdot \leftrightarrows H^+ + e^-,$$

where a proton in solution acts as an electron acceptor to donate a hydrogen atom to the platinum surface. In gas phase adsorption/desorption this reaction mode is not possible and hydrogen molecules are the reactive species:

$$H_2 \leftrightarrows 2H\cdot.$$

In addition, in the electrochemical case the adsorption is competitive with other species in solution, rather than the noncompetitive gas phase case. Nevertheless, the site energies on the platinum catalyst surfaces will be the same and the free energy differences between the two major hydrogen species (*3*, *7*, *9–14*) on these platinum surfaces ($\Delta\Delta G$ = 2.8 kcal) correspond to those values observed in gas phase perturbations (*3*, *9*).

The evaluation of catalyst surface areas, adsorption isotherms and heterogeneity/interaction effects on the platinum catalysts presented here is only possible because of the resolution capabilities of the electrochemical perturbation technique. It remains to be seen whether or not the gas phase thermal perturbation techniques can approach this resolution on similar materials. Because of the electronic nature of electrochemistry, it is limited to studying either unsupported metal catalysts or these metals supported on electronically conducting substrates; principally carbon. Refractory oxides used for supporting the highest surface area metal catalysts are inapplicable. The resolution of the electrochemical reaction rate/time profiles, however, more than compensates for the limitations in application.

REFERENCES

1. CVETANOVIĆ, R. J., AND AMENOMIYA, Y., *in* "Advances in Catalysis" (D. D. Eley, H. Pines and P. B. Weisz, Eds.), Vol. 17, p. 103. Academic Press, New York (1967).
2. REYNOLDS, T. W., *NASA Tech. Note* **D-4789,** (1968).
3. TSUCHIYA, S., AMENOMIYA, Y., AND CVETANOVIĆ, R. J., *J. Catal.* **19,** 245 (1970).
4. CZANDERNA, A. W., BIEGEN, J. R., AND KOLLEN, W., *J. Colloid Interface Sci.* **34,** 406 (1970).
5. STONEHART, P., *Electrochim. Acta* **13,** 1789 (1968).
6. STONEHART, P., KOZLOWSKA, H. A., AND CONWAY, B. E., *Proc. Roy. Soc., Ser. A* **310,** 541 (1969).

7. STONEHART, P., *Electrochim. Acta* **15**, 1853 (1970).
8. STONEHART, P., AND LUNDQUIST, J., *Electrochim. Acta* **18** (1973). (in press).
9. ABEN, P. C., VAN DER EIJK, H., AND OELDERIK, J. M., *in* "Fifth International Congress on Catalysis," Pap. No. 49, Palm Beach, 1972.
10. WILL, F. G., AND KNORR, C. A., *Z. Elektrochem.* **64**, 258 (1960).
11. WILL, F. G., *J. Electrochem. Soc.* **112**, 451 (1965).
12. ELEY, D. D., MORAN, D. M., AND ROCHESTER, C. H., *Trans. Faraday Soc.* **64**, 2168 (1968).
13. BREITER, M. W., *J. Electroanal. Chem.* **8**, 449 (1964).
14. BREITER, M. W., *Trans. Faraday Soc.* **62**, 2887 (1966).
15. BREITER, M. W., "Electrochemical Processes in Fuel Cells," p. 60. Springer-Verlag, New York, 1969.
16. MARVET, R. V., AND PETRII, O. A., *Electrokhimiya* **3**, 591 (1967).
17. STONEHART, P., AND ZUCKS, P. A., *Electrochim. Acta* **17**, 2333 (1972).
18. HANSEN, R. S., AND MIMEAULT, V. J., *in* "Experimental Methods in Catalytic Research" (R. B. Anderson, ed.), p. 217. Academic Press, New York, 1968.
19. FRANKLIN, T. C., NAITO, M., ITOH, T., AND MCCLELLAND, D. H., *J. Electroanal. Chem.* **27**, 303 (1970).
20. VOGEL, W. M., AND LUNDQUIST, J. T., *J. Electrochem. Soc.* **117**, 1512 (1970).
21. BETT, J. A. S., KINOSHITA, K., ROUTSIS, K., STONEHART, P., *J. Catal.* **29**, 160 (1973).
22. BENDANIEL, D. J., AND WILL, F. G., *J. Electrochem. Soc.* **114**, 909 (1967).